MULTI-DISCIPLINARY FAN ASSESSMENT WITH RESPECT TO BIRD STRIKE

S. A. Ritt [a], O. Kunc [a], N. Forsthofer [a], M. Schwämmle [a], S. Reitenbach [b]
German Aerospace Center DLR
[a] Institute of Structures and Design, Pfaffenwaldring 38-40, 70567 Stuttgart
[b] Institute of Propulsion Technology, Linder Höhe, 51147 Köln

Abstract

Bird strike is a dimensioning load case for the fan of aero engines. To analyse this dynamic loading, we work on automatically building FE models with sufficient degree of detail. This modelling includes both the rotating structure as well as non-rotating neighbouring structures. The pre- and post-processing is presented with focus on contributing to the overall engine design process of an example UHBR fan. This integrates into the development and collaboration platform GTlab.

Keywords

Bird Strike, Foreign Object Damage (FOD), Engine Design, Simulation, Process

1. INTRODUCTION

The design of gas turbine aero engines is a complex and multi-staged task spanning multiple disciplines across several levels of detail. contains a roughly simplified depiction of a possible overall workflow. Notably, in the first row, the level of detail increases from left to right whereas the workflow direction goes both ways. Foreign Object Damage (FOD) assessment is an example cause of such a flow of information from right to left: structural FOD tolerance requirements may cause geometrical changes so significant that previous assumptions on aerodynamics (e.g. flow path, pressure distribution) or structural properties (e.g. mass, modal behaviour) are no longer valid. In such a case, lower level designs need to be re-iterated. In the worst case, the suitability of the aircraft for certain missions might be affected, given the criticality of FOD.

For this reason, the goal is to assess the suitability of a fan with respect to bird strike as early as in the preliminary design phase, and to do so in an automated way.

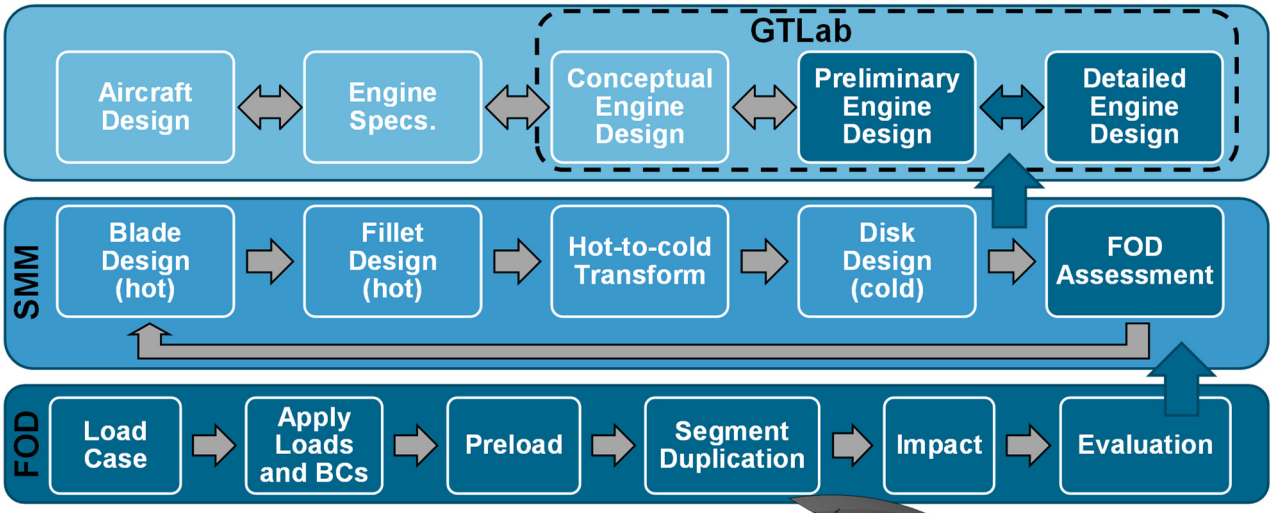

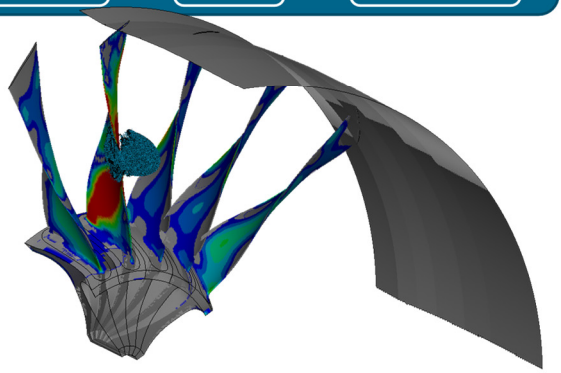

Figure 1: *Top*: conceptual process layout. The collaboration platform GTlab spans multiple domains and hosts sub-modules such as the Structural Mechanics Module (SMM). This module calls the FOD procedure and considers the corresponding results during the fan design process. *Right*: rotating fan segments during bird strike simulation and a quarter of the casing

doi: 10.25967/610231

2. OVERVIEW OF MULTIDISCIPLINARY FAN DESIGN PROCESS

Figure 1 exemplifies the overall engine design process (*first row*), some of its main structural mechanical steps (*second row*), and the FOD assessment as a sub-part of the latter (*third row*).

Here, the *first row* serves only the purpose of providing a broad overview. GTlab [1] is an integrative software framework designed for multidisciplinary, collaborative research in the field of propulsion technology. It supports the design and simulation of propulsion systems and individual components at different levels of detail throughout the entire product life cycle. The key strength of the framework is its consistent modularity. In addition to powerful core functions and core modules, GTlab offers the possibility to integrate specialised extension modules with plug-in capability to support a wide range of workflows covering different disciplines, from conceptual design through preliminary design to detailed design. Data acquisition throughout the design process in GTlab is handled by a centralised data processing unit, which enables efficient management of the complex data flow and large volumes of data transferred between disciplines and fidelity levels in a standardised manner.

In the *second row* of , a primary use-case of the Structural Mechanics Module (SMM) is sketched. It begins with aerodynamic design data as input (leftmost block). The intermediate steps preceding the FOD assessment constitute one possibility of designing a rotor disk fitting the aerodynamically optimised blade. Some details of this exemplary process will be given in Section 4.1. However, this part of the overall workflow is not the main interest in this context. Instead, this work focuses on the FOD assessment to which the SMM delivers inputs.

The *third row* outlines the FOD process, which is the primary contribution of this work. A result of the generated simulation model is shown in the lower part of . An in-depth description of this workflow will be provided in Section 4.2, with the example of an ultra-high bypass ratio (UHBR) engine fan.

3. UHBR ENGINE

For the present investigation an engine model of a generic ultra-high bypass-ratio (BPR ≈ 16) aircraft engine with an anticipated state of the art technology of 2028 was chosen [1]. This configuration has been developed within the DLR project PERFECT based on the B767 reference aircraft, which is expected to fill the gap in the current portfolio of aircraft at the best of future customer requirements.

The design process initiates with a 0D thermodynamic performance model and progressively incorporates 1D and 2D mid-fidelity tools for preliminary aerodynamic and structural assessments.

The application of this multi-disciplinary design process, which involved contributions from a wide range of different departments working in different disciplines across several iterative steps, resulted in a final engine design, at the target fidelity level of the PERFECT project, cf. Figure 2.

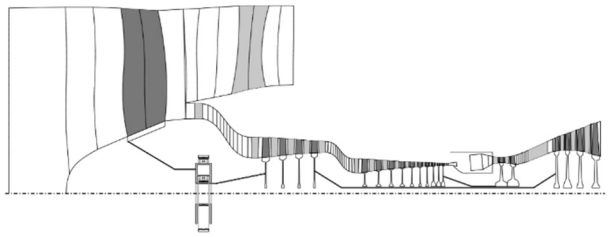

Figure 2: UHBR engine. The 3D model of this preliminary design contains the hot fan blade geometry and serves as input to the SMM. Notably, the fan disk is not yet designed at this stage.

The final configuration consists of a fan component driven by a planetary differential gear, which in turn is driven by a four-stage low-pressure turbine. The low-pressure compressor, also driven by the low-pressure shaft system, has four stages. On the high-pressure shaft is a ten-stage high-pressure compressor driven by a two-stage cooled high-pressure turbine.

The overall parameters of the final UHBR engine are shown in Table 1. The dimensioning operating points consist of the aerodynamic design point at cruise (CR) and three off-design points: The maximum take-off (MTO) and end of field (EOF) points represent the operating conditions that are subject to the highest mechanical and thermal loads. In addition, the Top of Climb (TOC) point is considered, which represents the highest corrected speeds and mass flows.

Table 1: Overall parameters of UHBR engine.

Parameter	Unit	CR	MTO	EOF	TOC
FN	[kN]	31	230	165	37
OPR	[-]	44.5	45.9	45.0	49.8
TSFC	[g/(kN s)]	13.5	6.2	8.8	13.9
T_3	[K]	795	968	971	864
T_4	[K]	1516	1893	1894	1674
T_{45}	[K]	1003	1269.6	1270	1113.7

4. FOD ASSESSMENT OF UHBR FAN BLISK

4.1. Input model

In this sub-section, we briefly describe the steps leading to the inputs of the FOD process. The purpose is to provide meaningful context and to highlight the integrative manner of the developed process environment. Sub-section 4.1.1 concerns the framework GTlab in general as well as lower-fidelity modules. The sub-sections 4.1.2 – 4.1.6 describe process steps provided by the SMM inside GTlab. The FOD process itself is described in 4.2.

4.1.1. Preliminary design

The design process invariably begins with a set of requirements captured in a Request for Proposal (RFP) or similar performance specification. In order to meet these criteria, a basic thermodynamic model is developed by means of the Performance module of GTlab that provides key insights into the characteristics of the engine throughout the design phase.

Based on this thermodynamic model, fast-running conceptual design tools are used to sketch the initial dimensions of the engine's core components. These initial dimensioning calculations are used not only to refine and recalibrate the thermodynamic model, but also to provide initial input for the subsequent design phase.

In the extended preliminary design phase, the geometric parameters of all major engine components are detailed. In the case of turbo components such as the fan, aspects include annulus geometry, blading, attachments, and possibly discs.

Although these detailed geometries result from preliminary design, they are comprehensive enough in order to be integrated into analyses of higher fidelity levels, such as Computational Fluid Dynamics (CFD) and Computational Structural Mechanics (CSM).

4.1.2. Fillet design

The bare rotor blade is enhanced by hub fillets. For this purpose, the GTlab GUI provides an interface to the fillet modelling capabilities of the underlying blade generator module [2] (“BladeGen”).

The initial fillet design is performed semi-automatically via user input of few main parameters, such as the height, width, and also the shape curve of the fillet. Scalar parameters can be defined at arbitrary control points along the profile of the blade, allowing for precise control of the fillet geometry.

A dedicated fillet optimisation sub-process will be provided by the SMM in the near future. It varies the parameters within user-defined boundaries, aiming for minimum mass while respecting stress constraints of a static load case.

4.1.3. Hot-to-cold transformation

A procedure similar to [3] is being implemented within the SMM. In essence, it approximates a solution of the inverse structural problem: how does the unloaded (“cold”) blade geometry have to be defined such that the aerodynamically optimised geometry (“hot”) is matched under the static loads of the aerodynamic design point? While this process is straight-forward for Finite Element (FE) meshes, it is quite complex for parametric descriptions or CAD geometry formats. The process currently under development will yield both CAD descriptions and parametric BladeGen designs.

4.1.4. Disk contour design

The design of the disk has significant influence on the stress distribution in the blade root, which is, according to [4], the most critical part for blade failure due to bird strike. Therefore, the disk must be designed before impact simulations can be conducted.

The disk geometry is constrained by available construction space and by structural mechanics. Therefore, the disk is designed by an optimisation process. The goal of the optimisation is to minimize the disk weight, while fulfilling stress and displacement restrictions. Limitations in construction space are a priori satisfied by the choice of the design parameter space.

The stress restriction is formulated as an inequality constraint. For isotropic metal disks, the maximum Mises stress can be evaluated against the tensile yield strength with an appropriate safety factor against bursting:

$$\sigma_{\mathrm{Mises}} \leq R_{\mathrm{p0,2}} * S_{\mathrm{burst}}$$

Displacement restrictions are used to prevent the disk from tilting or moving in axial direction. These have to be formulated as equality constraints. For tilting, the difference in radial displacement from leading edge to trailing edge at the blade hub is used whereas for axial displacement, only the blade hub leading edge point is evaluated:

$$\Delta r_{\mathrm{TE}} - \Delta r_{\mathrm{LE}} = 0$$

$$\Delta x_{\mathrm{LE}} = 0$$

The COBYLA algorithm, developed by Powell [2] and provided by the NLOpt [3] optimisation library for C++, is employed for the conduction of this optimisation task.

4.1.5. Meshing

The parametrised geometries need to be discretized for subsequent FE simulations. Dedicated meshing processes are utilised for blades and disks. In both cases, various sets of nodes, elements, and surfaces are identified during the meshing procedures for later use.

For *blade meshing*, a custom, structured, hexahedral mesher was implemented in GTLab. The 3D mesh is generated in four steps which are detailed in Figure 3.

In case of a rotor, it is beneficial to mesh the blade root finer than the tip in order to increase the stress resolution at and near the fillet section. This is accomplished via biasing of the radial meshing Step 4, c.f. Figure 3 (d).

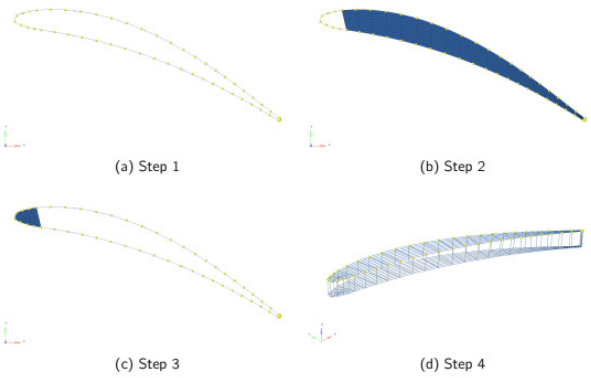

Figure 3: Blade meshing process. (a) 1D mesh of the contour as parametrised by the BladeGen format, (b) 2D mesh of the main interior profile, (c) mesh of leading edge and trailing edge regions (TE region is very small in this case), (d) connection of two adjacent quadrilateral profile meshes (“stacking”), defining the hexahedral elements.

For *disk meshing*, the open source mesher Gmsh [7] is used. First, the optimised 2D disk contour described in Section 4.1.4. is meshed with an unstructured 2D mesh using a quad-only Delaunay algorithm [8]. The 2D mesh is then rotationally extruded by $2\pi/N_{\mathrm{blades}}$ in order to generate a 3D hexahedral mesh of a single disk segment.

The design requirements may result in rotor stages with tightly arranged blades. This may generally lead to conflicts in case of linearly separated disk mesh sections (i.e. when

the disk segment is axially “cut” from the whole disk). Figure 4 illustrates this problem, where the rotational axis intersects two blade hub sections.

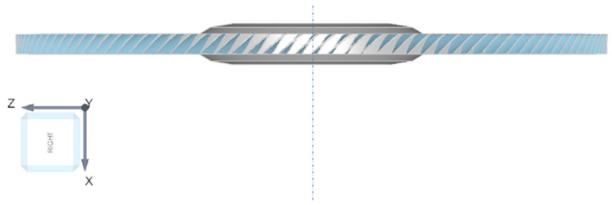

Figure 4: Rotor stage with a blade arrangement that causes the axis of rotation to intersect neighbouring blades.

To account for this case, an efficient disk mesh distortion algorithm has been implemented within the SMM. It distorts the disk mesh in circumferential direction such that the inclined and curved blade root is at the centre of the resulting disk segment, cf. Figure 5. This computation is always activated, regardless of the actual inter-blade clearance, because its runtime is negligible.

The algorithm initiates the disk mesh adaptation by computing a chord-defining spline for the rotor blade hub. A sufficiently high number of nodes are sampled along this spline to create a normalized trace. The angular distance of this trace from the mid-angle of the disk segment serves as the basis for the subsequent mesh distortion.

A precise distortion angle needs to be determined for each mesh node that may have a radial, an angular and an axial distance to the trace. Therefore, a connection line is constructed between each of the trace nodes and the extended x-axis of the engine. The x-intersections of these lines monotonically increase along the trace nodes.

Then, for each FE node, the closest member of this family of lines is found and its trace point is determined. This trace point possesses an angular distance to the mid-angle of the disk segment. This distance is first multiplied by an r-dependent factor, $0 \leq f(r_{FE}) \leq 1$, and then added to the angular coordinate of the FE node.

This way, the resulting circumferential distortion of the original mesh is zero at the axis of rotation, smooth, and affects all FE nodes including the ones with large axial distances to the blade, e.g. when they belong to flanges.

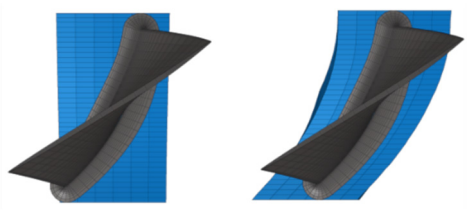

Figure 5: Disk mesh in blue color before (*left*) and after (*right*) circumferential distortion.

4.1.6. FE data management

Data management becomes increasingly challenging as the design transitions from the preliminary phase to the detailed phase. Whereas the preliminary design in GTlab is based on parametric descriptions of geometries, detailed analysis requires simulation-specific discretisation. For instance, a blade can be exactly described in the BladeGen format with ~100 – 200 parameters, depending on the level of detail. In contrast to this, an FE discretization of the same blade quickly exceeds 5000 nodes, each defined by 3 coordinates, and the corresponding mesh connectivity. The FE results then refer to the nodes or elements individually, multiplying the overall memory requirement by large factors.

In order to structure this FE data and to handle it efficiently, the VMAP standard [9],[10] is employed by the SMM.

The VMAP standard is based on the HDF5 file format and structures both model and result data in a straight-forward hierarchy. This (and other kinds of) HDF5 data are integrated into the GTlab framework such that the content is readily available to users and process developers alike. More information on the VMAP standard can be obtained from the official Standard Specifications [11]. Details on the integration of VMAP in GTlab and its usage in the SMM are being prepared for publication [12],[13].

As for the current work, the VMAP standard is the basis for the export of the FE model into the LS-DYNA format. Furthermore, parameters and other information necessary for the FOD process chain is directly output as re-usable python scripts.

4.2. FOD simulation

The simulation of the fan design under FOD shall be performed along with the airworthiness requirements as early as possible in a preliminary design phase, i.e. after the establishment of a fan geometry. This is to be remembered as the process described in this paper aims not to include details and design verifications typically developed during advanced product development. However, loading coming from the conceptual design (RPM e.g.) and description of the FOD in the airworthiness requirements can be studied.

4.2.1. Model data handling

The process for the FOD assessment is outlined in the third row of where the segment-based mesh (cf. Figure 5) is handed over from the preceding steps.

The data handling is realised by python, which is developed under an OSI-approved open source license [14], here in the version 3.8.17.

While a main simulation input structure is maintained, the adaptable process writes the input decks into separate include files, e.g. the part definitions dependable upon the number of segments created. The knowledge part of the process copies simulation input approved input decks into files, e.g. the control definitions. The concatenated main file is then launched with the solver LS-DYNA [15].

4.2.2. Material modelling for structural components

The modelling is based on given and available material data linked to the components by the assessment process.

The highest transient loading during a FOD of an engine occurs within the blade and disk of the fan. The material data of these components is therefore linked to a strain-rate and temperature dependent model [16] of Ti6Al4V4 [17].

4.2.3. Rotary load cases

The load definition is two-fold, first the rotary and non-transient loading of the components and second the

dynamic or impact loading by the foreign object (see following section).

The static pre-loading is currently the rotation resulting in centrifugal loads on rotor segments and the cyclic boundary conditions at the two corresponding disk faces, cf. Figure 6. Pressure loads on the blade will be considered in the future.

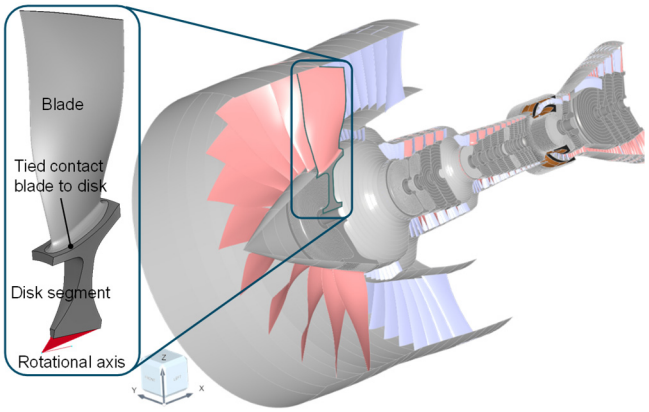

Figure 6 Segment based mesh to determine pre-loading.

These loads result in strains and stresses of blade and disk segment which are computed by means of a dynamic relaxation (DR) process realised by a non-linear implicit finite element analysis.

An impression of the resulting static deformation of the rotor segments is best visible by the effective nodal displacement plot which is given Figure 7.

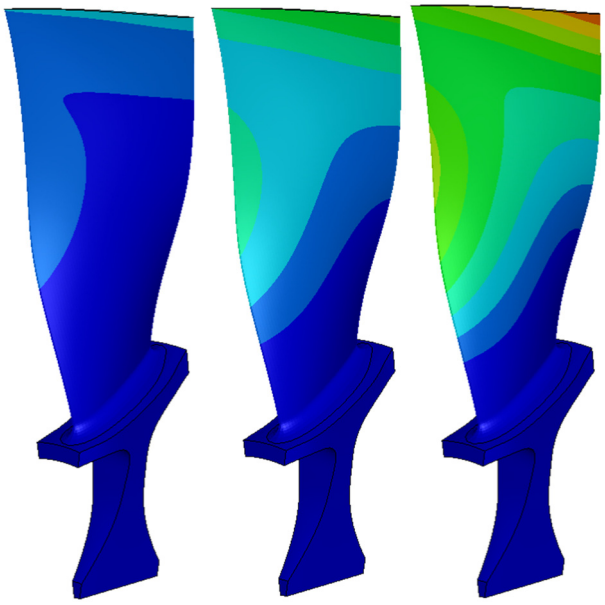

Figure 7: Three deformation plots of the fan rotor segment during dynamic relaxation.

4.2.4. FOD load cases

The process development is concentrated on the foreign object damage case and its airworthiness requirements. Bird strike represents the impact load case with the highest kinetic energy. This is obligatory for a future certification and is therefore of primary interest to this work.

As this paper concentrates on describing the process to include the FOD assessment into early design phases, only one load case in terms of foreign object is analysed. The single large bird along paragraph 800 (b) [18] is chosen for the analysis.

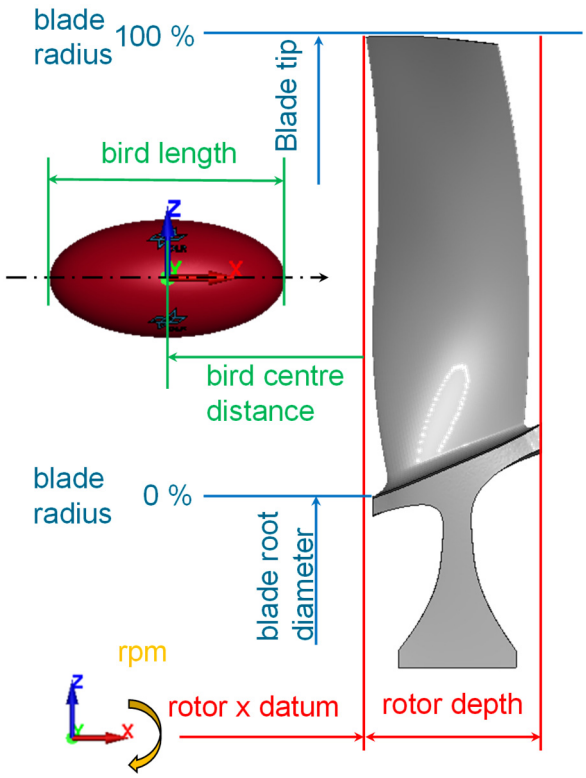

Figure 8: Positioning of bird model with respect to the rotating blade based on [19].

The number of rotor segments that are directly affected by the bird strike is computed from the rotational velocity of the fan in combination with both the length of the bird and its axial velocity.

4.2.5. Setup for assessment

While the rotational pre-loading is based on a single rotor segment, the FOD loading requires several rotating segments, as the foreign object introduces its total momentum into several rotating segments. Engaged by the momentum transfer, possible interaction between blades (induced clash, e.g.) needs to be covered in the modelling. Additionally, the rotor's movement plus the shape of the blades can lead to a centrifugal load on the fragmented bird masses. Hence, the casing with no penetration of bird particles is represented in the modelling, too. Currently, this tubular structure is modelled as rigid. Furthermore, the precise tip clearance is not yet modelled.

4.2.6. Applied Bird Model

The bird model was built up in terms of weight and applied axial velocity along the airworthiness requirements [18]. Accordingly, the weight shall be chosen in dependence upon the inlet throat diameter defined there. Given the diameter of the current fan, the maximum bird weight of 3.6 kg (8 lb) applies. For the considered load case, cf. Section 4.2.3, the axial velocity (parallel to the x-axis, Figure 8) is equal to 103 m/s (200 kts along [18][19]).

As the applied bird model is a kind of an artificial bird, a representative shape has to be selected for its modelling. Very common for engine application (rotating structures) are ellipsoidal shaped models while for structural application (static) cylinders with hemispherical caps are often applied. There have been comparisons of shape effects on fan blades [20]. A comparison of force-time histories of the given modelling with real bird tests under normal impact has been shown yet for the 1.0 kg bird at 110.2 m/s. The ellipsoidal (cf. Figure 8) and cylindrical shaped simulation model was first compared to artificial bird test and second to an identical measurement from real bird tests [21][22]. The application of simulation models [22] of 1.8 kg and 3.6 kg projectiles was shown for leading edges in [23] and the viability of the same shaped artificial birds in physical tests was confirmed between 110 and 165 m/s [24].

The simulation model of the bird in this work is built up by means of Smoothed Particle Hydrodynamics (SPH) as in [20][25]. The ellipsoidal shape is filled by 90790 uniformly distributed [25] particles.

4.2.7. FOD Process

The process is built upon the preloaded rotor segment which has to be completed prior to the foreign object loading. Given by the design with inlet diameter and RPM plus the chosen load case in terms of bird weight and its velocity, the required simulation time is calculated. The distance the projectile needs to travel through the rotor depends upon the projectile length and the rotor depth (cf. Figure 8). The simulation time is then calculated by this distance divided by the projectile velocity. Moreover, this time defines the number of segments which are directly affected by the impact. Subsequently, the process multiplies the segment, creates the necessary part information with types of elements and links to the material models. The boundary conditions and contact information are added.

In summary, the process is built upon three inputs: the pre-loaded rotor segment, a parameter set of the design, and a configuration data set incorporating the load case.

4.2.8. Processed evaluation

The evaluation is based upon binary output (BINOUT) of the explicit FE solver LS-DYNA [15]. The output is generated from the process execution.

The following evaluations are currently included:

1. Maximum values of (residual) plastic strain per segment
2. Axial tip displacement per blade
3. Clash / no clash per blade to blade force
4. Resultant force per blade

These four evaluations are visualised in a summary plot, cf. Figure 9. The maximum plastic effective strains of each segment are plotted against the property's elongation (see table 2B [17] for plate thicknesses between 4.76 and 101.60 mm). The three other evaluations are directly reflecting the binary results as described earlier in this section. The output sampling frequency of the results can be selected.

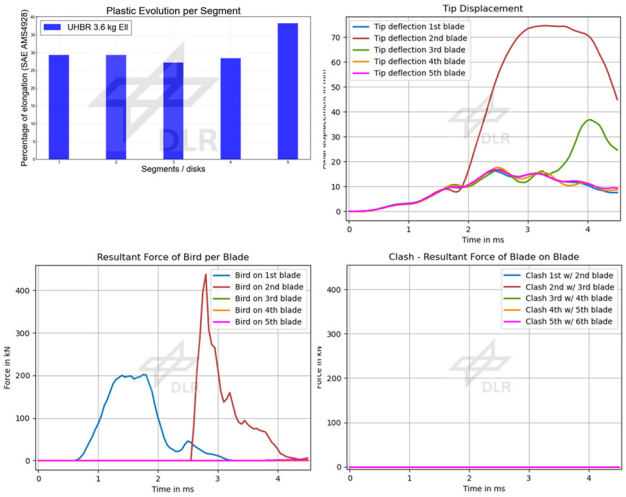

Figure 9: Result summary plot (in clock wise starting top left) for the bird impact with 3.6 kg at 103 m/s.

5. ASSESSMENT POSSIBILITIES

An example of assessment possibilities is given here by the comparison of the impact by the required 3.6 kg bird to the impact of the 1.8 kg bird model, while maintaining the point of impact and the velocity with 103 m/s, i.e. halving the momentum. The number of analysed segments is still based on the number determined in the 3.6 kg impact case.

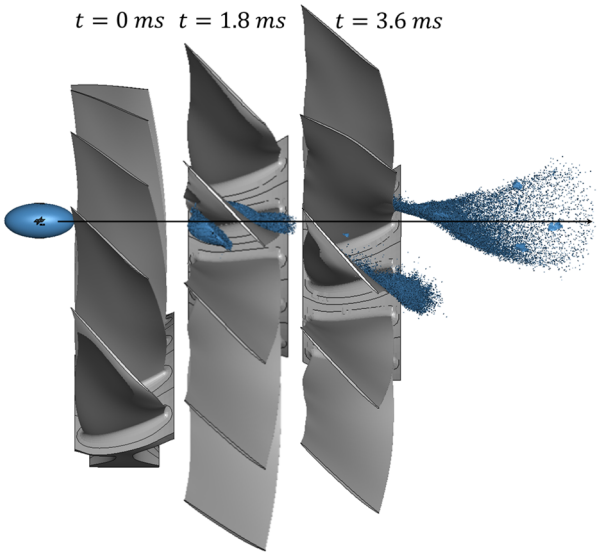

Figure 10: Three snapshots of the bird model traversing the rotor segments, which were rotated around the x-axis for better visibility.

The segmented view without the casing in Figure 10 gives an impression of how the bird model, here the 1.8 kg one, transfers its momentum to the blades. Consequently, the model bird is cut, here mainly into larger portions.

This division can be identified in the assessment graphs in Figure 11, too. In the upper row of the graphs, both for the 3.6 and the 1.8 kg bird the momentum is transferred to the first and second hit blade. The characteristics of the force-time history is similar for both cases while the peak load of the larger bird is approximately 36 % higher when the impact on the second segment is considered.

The axial tip deflection of all blades show a similar behaviour, except for the third blade which is deflected substantially less for the lighter bird.

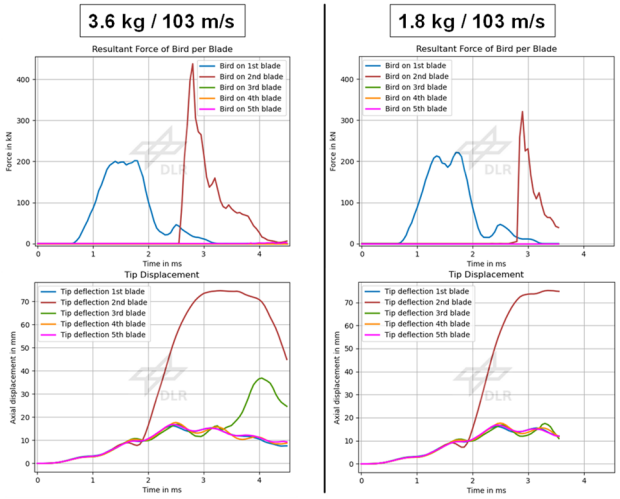

Figure 11: Comparison of a change in the FOD load case definition by reducing the bird weight from 3.6 kg to 1.8 kg

6. RESULTS AND CONCLUSION

A process to study foreign object damage on jet engine fan structures in a preliminary design process was built up. The foreign object considered here was a bird which was modelled in ellipsoidal shape by smoothed particle hydrodynamics. The data basis and how the foreign object damage was modelled on the rotating and non-rotating structure side in a process was outlined.

The generated results by the assessment process are summarised in a fact sheet after the completion of the simulation run.

This publication covers the current status of FOD assessment inside the conceptual and predesign activities within several institutes of the DLR. The assessment was shown here on a high bypass ratio engine fan rotor plus a part of the casing.

Other components like duct, spinner, deformable casing and stator rows were not considered yet.

The process with all steps has to be verified with other designs in order to show its stability and validity.

AUTHOR CONTRIBUTIONS

S. A. Ritt: Conception, all bird strike aspects from requirements, simulation and evaluation, programming and execution of the process of Sections 4.2 and later, writing and proof reading
O. Kunc: Conception, programming of the processes of Sections 4.1.2, 4.1.3, 4.1.6, testing and execution of all processes preceding 4.2, writing and proof reading
N. Forsthofer: Programming of the processes of Sections 4.1.3, 4.1.4, 4.1.5, writing
M. Schwämmle: Programming of the process of Section 4.1.5, writing
S. Reitenbach: Support with the GTlab framework and the UHBR model, writing

REFERENCES

[1] Vieweg M, Reitenbach S, et al. Collaborative Aircraft Engine Preliminary Design using a Virtual Engine Platform, Part B: Application. AIAA Scitech 2020 Forum.
[2] Voß C, Nicke E. Automatische Optimierung von Verdichterstufen. Technische Informationsbibliothek Hannover. 2008.
[3] Gaun L, Bestle D, Huppertz A. Hot-to-Cold CAD Geometry Transformation of Aero Engine Parts Based on B-Spline Morphing. Proceedings of the ASME Turbo Expo 2014: Turbine Technical Conference and Exposition.
[4] Johnson W, Mamalis A G, Gegenüberstellung statischer und dynamischer Schadens- und Deformationserscheinungen. Fortschr.-Ber. VDI-Z. Row 5 Nr. 32. VDI Publishing. 1977.
[5] Powell, M.J.D. (1994). A Direct Search Optimization Method That Models the Objective and Constraint Functions by Linear Interpolation. In: Gomez, S., Hennart, JP. (eds) Advances in Optimization and Numerical Analysis. Mathematics and Its Applications, vol 275. Springer, Dordrecht.
[6] Johnson S G. The NLopt nonlinear-optimization package. 2023. http://github.com/stevengj/nlopt .
[7] Geuzaine G, Remacle J-F. Gmsh: A three-dimensional finite element mesh generator with built-in pre-and post-processing facilities. In: 79 (Nov.2008).
[8] Remacle J-F et al. A Frontal Delaunay Quad Mesh Generator Using the Linf Norm. In: vol. 94. Jan. 2012, pp. 455–472.
[9] Gulati P. VMAP Enabling Interoperability in Integrated CAE Simulation Workflows. NWC21-205-b, Nafems World Congress 2021
[10] Wolf K. VMAP Standard and the VMAP Standards Community e.V.. NWC21-204-b, Nafems World Congress 2021
[11] VMAP Standard Specifications v1.0.0. https://vmap.vorschau.ws.fraunhofer.de/en/Specifications.html, last visited Oct 2023.
[12] Broecker M, Kunc O. Integration of large data based on HDF5 in a collaborative and multidisciplinary design environment, Part A: Methodology and Implementation. AIAA SciTech, 2024.
[13] Kunc O, Broecker M. Integration of large data based on HDF5 in a collaborative and multidisciplinary design environment, Part B: Application to Structural Mechanics of Gas Turbine Engines. AIAA SciTech, 2024.
[14] Python Software Foundation. Python programming language. https://www.python.org/, last visited Oct 23 2023.
[15] Ansys. LS-DYNA - A Program for Nonlinear Dynamic Analysis of Structures in Three Dimensions. R14.0. 12.12.2022.
[16] FAA. An Evaluation of MAT_224 for Simulation of Impact and Failure Part 1: A Scaling Approach for Modeling AMS 4911 Titanium Plates with Different Thicknesses and Properties. Final Report. October 2018.
[17] SAE. Titanium Alloy, Sheet, Strip, and Plate 6Al - 4V Annealed. AMS 4911R. 2019-12.
[18] EASA. Certification specification and acceptable means of compliance for engines (CS-E). Amendment 6. 24.06.2020.

[19] FAA. Bird Ingestion Certification Standards, Advisory circular. AC33.76-1B. 03.04.2023
[20] Vignjevic R, Orlowsky M, de Vuyst T, Campbell J C. A parametric study of bird strike on engine blades. International Journal of Impact Engineering 60 (2013) 44-57
[21] Ritt S A, Hoefer F, Oswald J, Schlie D. Drone and bird loading, ERF. 2001
[22] Ritt S A, Vinot M. Impact Studies with Reduced Size Aircraft Stabiliser Demonstrators Including Hybrid Laminar Flow Control Technology. Clean Sky 2 Technology Progress, 24.-25.03.2021, Madrid, Spain / virtual.
[23] Ritt S A, Schlie D. Comparative studies of bird strike by dummy tests. 2. Dummy.Crashtest.Konferenz. Muenster, Germany. 08.-09.09.2022.
[24] Ritt S A. Clean Sky 2 Deliverable D1.4.1.4-28 - Impact test campaign progress report on complex HTP Segments. Project report, 32 pages. 22.12.2022.
[25] Budgey R. The development of a substitute artificial bird by the IBRG for use in aircraft component testing. IBSC25, Amsterdam. 17.21.04.2000.
[26] Siemann M H, Ritt S A. Novel particle distributions for SPH bird-strike simulations. Computer Methods in Applied Mechanics and Engineering. Volume 343, 2019, 746-766.